JOURNAL OF AIRCRAFT
Vol. 38, No. 4, July–August 2001

Transonic Flow of Moist Air Around a Thin Airfoil with Equilibrium Condensation

Jang-Chang Lee* and Zvi Rusak†
Rensselaer Polytechnic Institute, Troy, New York 12180-3590

The two-dimensional and steady transonic flow of atmospheric moist air with equilibrium condensation around a thin airfoil is investigated. The study is based on an asymptotic analysis and numerical simulations. A small-disturbance model is developed to explore the nonlinear interactions between the near-sonic speed of the flow, the small thickness ratio and angle of attack of the airfoil, and the small amount of mass of water vapor in the air. The condensation process of water vapor in the air is assumed to be isentropic. The similarity parameters that govern the flow problem are provided. The flowfield may be described by a modified transonic small-disturbance (TSD) equation that includes parameters that are related to the condensation process. Murman and Cole's method (Murman, E. M., and Cole, J. D., "Calculation of Plane Study Transonic Flows," *AIAA Journal*, Vol. 9, No. 1, 1971, pp. 114–121.) is used for the numerical solution of the modified TSD problem. The results show that the flow of moist air is similar to the flow of dry air with an effective freestream Mach number that is greater than the freestream Mach number of moist air. The present approach is used to study the aerodynamic performances of airfoils in atmospheric transonic flight with humidity.

Nomenclature

a_∞	=	speed of sound of freestream
B	=	airfoil shape function
Ca	=	airfoil camber line function
C_{pa}, C_{va}	=	specific heat at constant pressure and volume of dry air
C_{pv}, C_{vv}	=	specific heat at constant pressure and volume of water vapor
$\tilde{C}_p$	=	constant, C_{pv}/C_{pa}
$\tilde{C}_v$	=	constant, C_{vv}/C_{va}
c	=	airfoil's chord
c_p	=	pressure coefficient
$F_{u,l}$	=	shape functions of airfoil's surfaces
g	=	condensate mass fraction, m_L/m
$H(z)$	=	Heaviside function
h_f	=	specific enthalpy of saturated water liquid
h_{fg}	=	latent heat
h_g	=	specific enthalpy of saturated water vapor
h_L	=	specific enthalpy of condensate
h_T	=	specific total enthalpy
K	=	transonic similarity parameter
$\bar{K}$	=	modified transonic similarity parameter
K_ω	=	moist air similarity parameter
M	=	frozen Mach number
$M_{\infty,\max}$	=	Mach number of maximum lift coefficient
$\bar{M}_\infty$	=	effective freestream Mach number
m	=	mass of a fluid particle, $m_a + m_v + m_L$
m_L	=	mass of condensate in a fluid particle
p	=	pressure
$\bar{p}$	=	nondimensional pressure, p/p_∞
R	=	moist air gas constant
$\bar{R}$	=	universal gas constant
S	=	supersaturation ratio, p_v/p_g
s	=	specific entropy
s_f	=	specific entropy of saturated water liquid
s_g	=	specific entropy of saturated water vapor
s_L	=	specific entropy of condensate
T	=	temperature
$\bar{T}$	=	nondimensional temperature, T/T_∞
t	=	thickness distribution of airfoil
U_∞	=	freestream velocity
u	=	axial velocity
V	=	volume of a fluid particle
v	=	transverse velocity
x, y	=	Cartesian space coordinate
$\bar{x}$	=	nondimensional streamwise coordinate
$\tilde{y}$	=	stretched normal coordinate
γ_a	=	specific heats ratio of dry air, 1.4
ϵ	=	thickness ratio of airfoil
Θ	=	θ/ϵ
θ	=	airfoil angle of attack
μ	=	molecular weight
ρ	=	density
$\bar{\rho}$	=	nondimensional density, ρ/ρ_∞
Φ	=	relative humidity, p_v/p_g
ϕ_1	=	velocity perturbation potential
χ	=	humidity ratio or mixing ratio
ψ	=	stream function
ω	=	local initial specific humidity, $(m_v + m_L)/m$

Subscripts

a	=	dry air
f	=	saturated water liquid
g	=	saturated water vapor
v	=	water vapor
∞	=	freestream

Received 3 July 2000; revision received 24 August 2000; accepted for publication 9 October 2000.

*Postdoctorate Associate, Department of Mechanical Engineering, Aeronautical Engineering and Mechanics. Member AIAA.

†Professor, Department of Mechanical Engineering, Aeronautical Engineering and Mechanics. Senior Member AIAA.

I. Introduction

THE air in the lower levels of the atmosphere is a heterogeneous medium that typically contains humidity. The air is considered as a mixture of perfect gases that is composed of dry air and water vapor. The dry air does not condense, but the water vapor can change its phase to liquid or ice.[1] Flight in moist air may create in certain regions of the flowfield around the wings the thermodynamic conditions for the condensation of water vapor. Pictures of such condensation phenomena around flying airplanes at transonic speeds can be found, for example, in the work of Campbell et al.[2] and Gay.[3] These examples show small and large regions in the flowfield

around airplanes where water liquid droplets exist. Those regions are similar in their size to the supersonic regions of the flow around the airplane. It is also expected that the heat release by the condensation process to the air can affect the flow properties and the aerodynamic performance of the wings.[4,5] Studying the dynamics of moist air around airfoils is of basic scientific interest and is useful for technical applications such as the design of airplane wings and of helicopter blades.

The transonic flow of moist air has been studied by Head,[6] Wegener and Mack,[7] Schmidt,[8] Zierep,[9,10] Jordan,[11] Hall,[12] Campbell et al.,[2] Schnerr and Dohrmann,[4,5] and Schnerr and Mundinger.[13] It was found that in most relevant cases of transonic flows moist air reaches the saturation conditions and then the condensation of water vapor in the air may occur.

There are two possible limit types of condensation processes (see Wegener[14]). One possible type of behavior is a nonequilibrium process. This process typically occurs in fast flow expansions of purified vapors around airfoils in internal chambers. In this process, the water vapor remains supersaturated even though equilibrium saturation conditions are already achieved. The supersaturation ratio $S = p_v/p_g(T) > 1$ (which is an extension of the the concept of relative humidity into the saturation region, see Zettlemoyer[15] and Abraham[16]) may increase much above 1 ($S \gg 1$) without condensation. Condensation starts only at a critical state where the liquid droplets reach their critical size. This state is known as the supersaturation state. A significant spontaneous nucleation of water droplets takes place, known as homogeneous condensation. The second type of condensation is an equilibrium process, which typically occurs in flows where there are large numbers of foreign nuclei, that is, dust, aerosols, and ions, or when the phase changes are relatively slow. In this process the condensation starts immediately as water vapor reaches the saturation conditions. It may be modeled as an isentropic process that evolves according to the local flow properties. The various studies show that the nonequilibrium process takes place in transonic wind tunnels operating with atmospheric moist air. On the other hand, the equilibrium process usually occurs in atmospheric transonic flight. In this paper, we focus on atmospheric transonic flows of moist air around a thin airfoil with equilibrium (isentropic) condensation.

Wegener and Mack[7] investigated the general effect of heat transfer to or from the flow on the behavior of shock waves in a transonic or supersonic flow. They demonstrated the possible appearance of condensation shock waves and of exothermic jumps in subsonic flows in addition to modified regular shock waves with either condensation or vaporization.

Zierep[9] suggested a transonic small-disturbance (TSD) model equation to describe the flow around a thin airfoil. In this model, a prescribed heat source term was used to represent the heat addition to the flow. An approximate solution of this problem for various prescribed values of the heat input were proposed. It was found that there is a critical heat input above which no steady-state solution exists. Zierep[9] also predicted a possible reduction of the airfoil's drag as a result of a heat input in the supersonic part of the flowfield. Schnerr and Mundinger[13] used Zierep[9] TSD model together with prescribed distributions of heat sources. They suggested similarity parameters related to internal heat addition. They also studied the changes in the aerodynamic lift and drag of airfoils resulting from the heat addition.

Schnerr and Dohrmann[4,5] used numerical simulations to study transonic flows of moist air around airfoils. Their model was based on the inviscid flow equations of motion with a heat addition term, which is related to the condensation. They computed both nonequilibrium and equilibrium condensation processes. Depending on the airfoil's geometry and different supply conditions, they showed significant variations of the lift and pressure drag of airfoils as the relative humidity at the freestream flow is varied. Schnerr and Dohrmann[5] also showed significant differences in the resulting pressure distributions for the two condensation processes.

The previous studies demonstrated the complicated nature of transonic flows of moist air around airfoils. The structure of these flowfields is not similar to that of a dry air flow and results in important changes in the aerodynamic performances of the airfoils. An asymptotic approach that reduces the flow and condensation equations to simpler set of model equations may help to clarify the complicated compressible flow physics of moist air.

Recently, Rusak and Lee[17] and Lee and Rusak[18] developed a TSD model equation together with simplified ordinary differential equations for the nonequilibrium and homogeneous condensation of moist air at transonic speeds. They described the parameters that govern the flow and condensation processes. The similarity rules were demonstrated by numerical simulations. The effects of varying the parameters were studied by Lee.[19] Significant changes in the flow properties and in the pressure distributions around airfoils as a result of the energy supply by condensation were found.

The approach[17–19] is extended in this paper to describe the transonic flow of moist air with equilibrium condensation around a thin airfoil. The mathematical model of the flow and condensation problem is described in Sec. II. The asymptotic analysis in Sec. III relates between the near-sonic speed of the flow, the small thickness and angle of attack of the airfoil, and the small amount of water vapor in the air. It results in the similarity parameters that govern the flow problem. Also, the flowfield can be described by a modified TSD equation. This approach extends the classical TSD problem for dry air[20] and the works of Zierep[9] and Schnerr and Mundinger[13] where the heat addition is prescribed. The Murman and Cole[21] method is used to solve the modified TSD equation numerically. The results in Sec. IV show that the flow of atmospheric moist air is similar to the flow of dry air with an increased (effective) freestream Mach number. The results describe the effects of equilibrium condensation in atmospheric moist air on the aerodynamic performance of airfoils.

II. Mathematical Model

A steady, inviscid, and two-dimensional stream of moist air around a thin airfoil is considered (Fig. 1). The freestream flow ahead of the airfoil is assumed to be uniform at pressure p_∞, density ρ_∞, temperature T_∞, and relative humidity $0 \le \Phi_\infty \le 100\%$ [note that the relative humidity Φ is a thermodynamic property that represents the ratio of the water vapor pressure p_v to the saturation pressure of water vapor $p_g(T)$ at a given temperature T]. The freestream speed U_∞ is in the axial direction only and is close to the isentropic speed of sound a_∞ of the freestream moist air at the given conditions. The frozen freestream Mach number $M_\infty = U_\infty/a_\infty \sim 1$. The freestream speed of sound is $a_\infty = \sqrt{(\gamma_\infty R_\infty T_\infty)}$. Here γ_∞ is the ratio of specific heats of moist air:

$$\gamma_\infty = \frac{C_{p\infty}}{C_{v\infty}} = \frac{(1-\omega_\infty)C_{pa} + \omega_\infty C_{pv}}{(1-\omega_\infty)C_{va} + \omega_\infty C_{vv}} = \gamma_a \frac{1-\omega_\infty + \omega_\infty \tilde{C}_p}{1-\omega_\infty + \omega_\infty \tilde{C}_v} \tag{1}$$

and $R_\infty (= \bar{R}/\mu_\infty)$ is the specific gas constant of moist air. The apparent molecular weight of the freestream moist air, μ_∞, is given by $1/\mu_\infty = (1-\omega_\infty)/\mu_a + \omega_\infty/\mu_v$, where μ_a and μ_v are the molecular weights of dry air and water, respectively. The initial specific humidity at the freestream state (the ratio of the mass of water

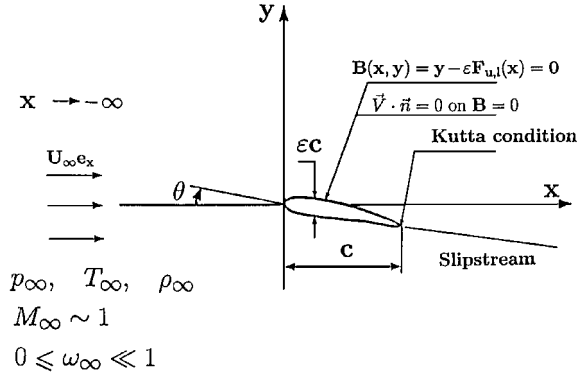

Fig. 1 Airfoil flow problem.

vapor in a particle to the mass of moist air in the particle) is $\omega_\infty = [m_v/(m_a+m_v)]_\infty = \chi_\infty/(1+\chi_\infty)$, where the humidity ratio (or the mixing ratio) at the freestream flow is

$$\chi_\infty = \left.\frac{m_v}{m_a}\right|_\infty = \frac{\mu_v}{\mu_a}\frac{p_g(T_\infty)\Phi_\infty}{p_\infty - p_g(T_\infty)\Phi_\infty} \tag{2}$$

Here $p_g(T)$ is the saturation pressure of water vapor. Also, $\gamma_a (= C_{pa}/C_{va})$ is the ratio of specific heats of dry air, where C_{pa} and C_{va} are the specific heats of dry air at constant pressure and volume, respectively. C_{pv} and C_{vv} are the specific heats of water vapor when it is approximated as a perfect gas. $\tilde{C}_p = C_{pv}/C_{pa}$ and $\tilde{C}_v = C_{vv}/C_{va}$. In the atmospheric conditions we always have $p_g(T_\infty) \ll p_\infty$. This means that each particle of moist air contains only a small amount of mass of water vapor, $0 \le \omega_\infty \ll 1$. Also, we assume that no condensation takes place at the freestream state. This means that the condensate mass fraction $g_\infty = [m_L/m]_\infty = 0$ as $x \to -\infty$. Also, there is no injection of water vapor or liquid to the flow through the airfoil's surfaces.

The shape of the thin airfoil is given by

$$B(x, y) = y - \epsilon c F_{u,l}(x/c) = 0 \qquad \text{for} \qquad 0 \le x/c \le 1 \tag{3}$$

where $0 < \epsilon \ll 1$. The shape functions $F_{u,l}(x/c)$, which represent the upper and lower surfaces of the airfoil, are given by

$$F_{u,l}(x/c) = Ca(x/c) \pm t(x/c) - \Theta(x/c) \quad \text{for} \quad 0 \le x/c \le 1 \tag{4}$$

where $Ca(x/c)$ describes the camber line, $t(x/c)$ is the thickness distribution, and $\Theta = \theta/\epsilon$, where θ is the angle of attack. Also, $t(0) = t(1) = 0$ and $Ca(0) = Ca(1) = 0$.

The conservation equations of mass, momentum, and energy are used to represent the compressible flowfield of moist air around the airfoil:

$$(\rho u)_x + (\rho v)_y = 0 \tag{5}$$

$$(\rho u^2 + p)_x + (\rho u v)_y = 0 \tag{6}$$

$$(\rho u v)_x + (\rho v^2 + p)_y = 0 \tag{7}$$

$$(\rho h_T u)_x + (\rho h_T v)_y = 0 \tag{8}$$

where p is the local pressure. The specific total enthalpy is $h_T = \frac{1}{2}(u^2+v^2) + (m_a/m)h_a + (m_v/m)h_v + (m_L/m)h_L$, where m_a, m_v, and m_L are the mass of dry air, of water vapor, and of water liquid in a fluid particle, respectively. Also, following Ref. 22, we assume that $h_a = C_{pa}T$, $h_v \sim h_g(T) = C_{pv}T$ and $h_L \sim h_f(T) = h_g(T) - h_{fg}(T)$. Here h_a, h_v, and h_L are the dry air, the water vapor, and the condensate specific enthalpies, respectively, and h_{fg} is the latent heat resulting from the condensation of water vapor into liquid.

We define the local density of a fluid particle as $\rho = \rho_a + \rho_v + \rho_l$. The partial density of dry air ρ_a is the mass of dry air in a fluid particle over the particle's volume. The partial density of water vapor ρ_v is the mass of water vapor in a fluid particle over the particle's volume. The partial density of condensate ρ_l is the mass of condensate in a fluid particle over the particle's volume.

The local initial specific humidity is defined as $\omega = (m_v + m_L)/m$, where ω is the small amount of mass of water vapor in the air and typically $0 \le \omega \ll 1$. The local condensate mass fraction is defined as $g = m_L/m$ and $0 \le g < \omega$. We find that $h_T = \frac{1}{2}(u^2+v^2) + [(1-\omega)C_{pa} + \omega C_{pv}]T - g h_{fg}$. Using Eqs. (5) and (8), it can be shown that the specific total enthalpy h_T is constant along a constant stream function line ψ where $\psi_y = \rho u$ and $\psi_x = -\rho v$. Therefore, the energy Eq. (8) becomes an algebraic relation:

$$\tfrac{1}{2}(u^2+v^2) + [(1-\omega)C_{pa} + \omega C_{pv}]T - g h_{fg} = h_T(\psi) \tag{9}$$

The equation of state for a thermally perfect gas is also considered, relating between the local thermodynamic properties of moist air:

$$p = (\bar{R}/\mu)\rho T \tag{10}$$

where μ is the local apparent molecular weight of moist air, $1/\mu = (1-\omega)/\mu_a + (\omega - g)/\mu_v$.

Equations (5–7), (9), and (10) describe the flowfield of moist air including the heat supply caused by the condensation process, which appears in the energy Eq. (9). Notice that the heat source term vanishes in flow regions with no condensation.

Following Wegener and Mack[7] (page 367), the mass of dry air (the inert carrier gas) remains constant, and the condensate grows at the expense of the water vapor. Using this argument, the continuity Eq. (5), the relation $\rho = \rho_a/(1-\omega)$, and the uniform flow conditions at the freestream state, we find that the initial specific humidity is constant all over the field, that is, $\omega = \omega_\infty$ for every (x, y). This result is also correct across any shock wave that may appear in the flow.[19] It reflects the conservation of mass of water at any point in the flowfield.

Also, from the far-field conditions, we find that in the energy Eq. (9) $h_T(\psi)$ is constant all over the field:

$$\tfrac{1}{2}(u^2+v^2) + C_{p\infty}T - g h_{fg} = \tfrac{1}{2}U_\infty^2 + C_{p\infty}T_\infty \tag{11}$$

for every (x, y). $C_{p\infty} = (1-\omega_\infty)C_{pa} + \omega_\infty C_{pv}$. This result is also correct across any shock wave that may appear in the flow.[19] It reflects the conservation of the specific total enthalpy at any point in the flowfield.

To compute the condensate mass fraction g, we assume that the equilibrium condensation process is isentropic, that is, the specific entropy of moist air is constant:

$$s = (1-\omega)s_a + (\omega - g)s_v + g s_L = \text{const} \tag{12}$$

and when $g > 0$, the pressure of the mixture of water vapor and liquid in each particle is the saturation pressure of the local temperature, that is, the vapor pressure is $p_v = p_g(T)$. In Eq. (12), s_a, s_v, and s_L are the specific entropies of dry air, of water vapor, and of condensate, respectively. These are found from the local thermodynamic properties of the flow. From the freestream condition, $g \to 0$, $s_a \to s_{a\infty}$, and $s_v \to s_{v\infty}$ as $x \to -\infty$, we find that

$$(1-\omega_\infty)s_a + (\omega_\infty - g)s_v + g s_L = (1-\omega_\infty)s_{a\infty} + \omega_\infty s_{v\infty} \tag{13}$$

The entropy change of dry air with respect to the two states[22] is

$$s_a - s_{a\infty} = C_{pa}\,\ell n(T/T_\infty) - R_a\,\ell n(p_a/p_{a\infty}) \tag{14}$$

where C_{pa} and R_a are the specific heat at constant pressure and the gas constant of dry air. Because there is no chemical reaction in the mixture, we have

$$p_a/p = n_a/(n_a+n_v) = p_{a\infty}/p_\infty \tag{15}$$

where $p = p_a + p_v = (n_a+n_v)\bar{R}T/V$, $p_a = n_a\bar{R}T/V$, and $p_v = n_v\bar{R}T/V$ are used. Here, n_i and V are the number of moles of each mixture component and the volume of the mixture at temperature T. When Eqs. (14) and (15) are used, the specific entropy change of dry air is

$$s_a - s_{a\infty} = C_{va}\,\ell n(p/p_\infty) - C_{pa}\,\ell n(\rho/\rho_\infty) \tag{16}$$

Also, we assume that $s_v \sim s_g$ and $s_L \sim s_f$ (Moran and Shapiro[22]) where s_g and s_f are the specific entropies of saturated water vapor and liquid. Therefore, from Eqs. (13) and (16), we have

$$g = \frac{(1-\omega_\infty)[C_{va}\,\ell n(p/p_\infty) - C_{pa}\,\ell n(\rho/\rho_\infty)]}{s_g(T) - s_f(T)} + \frac{\omega_\infty[s_g(T) - s_{v\infty}]}{s_g(T) - s_f(T)} \tag{17}$$

when the right-hand side of Eq. (17) is positive and $g = 0$ when the right-hand side of Eq. (17) is negative.

The system of flow Eqs. (5–7), (9), and (10) coupled with the condensation Eq. (17) describes the flowfield of a steady and inviscid moist air with equilibrium condensation. The solution of these

equations should satisfy the condition of the tangency of the flow on the airfoil surface:

$$uB_x + vB_y = 0 \qquad \text{on} \qquad B(x, y) = 0 \tag{18}$$

Also, disturbances to the uniform flow must die out at upstream infinity:

$$u \to U_\infty, \qquad v \to 0, \qquad \rho \to \rho_\infty, \qquad p \to p_\infty, \qquad g \to 0$$
$$\text{for every } y \quad \text{as} \quad x \to -\infty \tag{19}$$

The Kutta condition must be satisfied at a sharp trailing edge. To get a one-valued flowfield, the (x, y) plane is cut along the slipstream that leaves the trailing edge to infinity.

To study the transonic flow of moist air around a thin airfoil, the flow and condensation properties are approximated by asymptotic expansions in the limit where the thickness ratio of the airfoil is small ($\epsilon \to 0$), the frozen freestream Mach number is near 1 ($M_\infty \to 1$), and the initial specific humidity is also small ($\omega_\infty \to 0$).

III. Asymptotic Analysis

In the case of a transonic flow of moist air around a thin airfoil, the freestream flow is characterized by a frozen Mach number that is close to 1 and by small values of the initial specific humidity (by small amount of mass of water vapor in the air). It is expected that the thin airfoil creates in most of the flowfield only slight perturbations to the uniform flow properties, except for a small region near the nose of the airfoil (on the order of ϵ^2) where the perturbations are large. To describe the nonlinear interactions between the various perturbations, we may consider the following expansions[20]:

$$\tilde{y} = \epsilon^{\frac{1}{3}} y/c, \qquad \omega_\infty = \epsilon^{\frac{4}{3}} K_\omega, \qquad M_\infty^2 = 1 - K\epsilon^{\frac{2}{3}}$$

and

$$\bar{\rho} = \rho/\rho_\infty = 1 + \epsilon^{\frac{2}{3}}\bar{\rho}_1 + \epsilon^{\frac{4}{3}}\bar{\rho}_2 + \cdots$$
$$\bar{p} = p/p_\infty = 1 + \epsilon^{\frac{2}{3}}\bar{p}_1 + \epsilon^{\frac{4}{3}}\bar{p}_2 + \cdots$$
$$\bar{T} = T/T_\infty = 1 + \epsilon^{\frac{2}{3}}\bar{T}_1 + \epsilon^{\frac{4}{3}}\bar{T}_2 + \cdots$$
$$\bar{u} = u/U_\infty = 1 + \epsilon^{\frac{2}{3}}\bar{u}_1 + \epsilon^{\frac{4}{3}}\bar{u}_2 + \cdots$$
$$\bar{v} = v/U_\infty = \epsilon\bar{v}_1 + \epsilon^{\frac{5}{3}}\bar{v}_2 + \cdots, \qquad \bar{g} = g/\omega_\infty = \bar{g}_1 + \cdots \tag{20}$$

The substitution of Eq. (20) into the flow equations gives after some algebra (see also Rusak and Lee[17])

$$\bar{T}_1 = -(\gamma_a - 1)M_\infty^2\phi_{1\bar{x}}, \qquad \bar{p}_1 = -\gamma_a M_\infty^2\phi_{1\bar{x}} \tag{21}$$

and an extended Kármán–Guderley equation for the solution of the velocity-perturbation potential ϕ_1:

$$\left[K - (\gamma_a + 1)M_\infty^2\phi_{1\bar{x}}\right]\phi_{1\bar{x}\bar{x}} + \phi_{1\bar{y}\bar{y}} = \bar{g}_{1\bar{x}}K_\omega\left[\frac{h_{fg}(T_\infty)}{C_{pa}T_\infty} - \frac{\mu_a}{\mu_v}\right] \tag{22}$$

where $\bar{x} = x/c$, $\tilde{y} = \epsilon^{1/3}y/c$ is the stretched vertical coordinate, $\bar{u} = \phi_{1\bar{x}}$, and $\bar{v} = \phi_{1\bar{y}}$. Also, K is the classical transonic similarity parameter that represents the deviation of the freestream Mach number from 1 in terms of the small ϵ. The parameter K_ω is the moist air similarity parameter, which reflects the small amount of mass of water vapor in moist air in terms of the airfoil's small thickness ratio. The boundary conditions for solving Eq. (22) are the linearized tangency condition along the airfoil's chord, the Kutta condition at the trailing edge, and the decay of the perturbations in the far field:

$$\phi_{1\bar{y}}(\bar{x}, 0^\pm) = F'_{u,l}(\bar{x}) \qquad \text{for} \qquad 0 \le \bar{x} \le 1$$
$$\phi_{1\bar{x}}(1, 0^+) = \phi_{1\bar{x}}(1, 0^-)$$
$$\phi_{1\bar{x}}, \phi_{1\bar{y}} \to 0 \quad \text{as} \quad \bar{x} \to -\infty \tag{23}$$

The condensate mass fraction $\bar{g}_1$ in Eq. (22) is calculated according to Eq. (17). When Eq. (20) is used, it can be shown that the change in the specific entropy of dry air is $\mathcal{O}(\epsilon^2)$. Therefore, its effect can be neglected in Eq. (17). Finally, we find that

$$\bar{g}_1 = \frac{s_g(T) - s_{v\infty}}{s_g(T) - s_f(T)} = \frac{s_g(T_\infty) - s_{v\infty}}{s_{fg}(T_\infty)} + \epsilon^{\frac{2}{3}}\frac{\bar{T}_1 T_\infty}{s_{fg}(T_\infty)}\left(\frac{ds_g}{dT}\right)_\infty\left[1 - \frac{s_g(T_\infty) - s_{v\infty}}{s_{fg}(T_\infty)}\right] \tag{24}$$

when the right-hand side of Eq. (24) is positive and $\bar{g}_1 = 0$ when the right-hand side of Eq. (24) is negative. Note that the condensate mass fraction $\bar{g}_1$ is related to the change of temperature in the flow. Also, when $\bar{g}_1 > 0$, the pressure of the mixture of water vapor and liquid in each particle is the saturation pressure of the local temperature, that is, the vapor pressure is $p_v = p_g(T_\infty\bar{T})$, where $\bar{T} = 1 - \epsilon^{2/3}(\gamma_a - 1)M_\infty^2\phi_{1\bar{x}}$.

Because $(ds_g/dT)_\infty < 0$ for every T_∞ (see Ref. 22), $\bar{g}_1$ is generated only when the temperature decreases below a certain value, that is,

$$\epsilon^{\frac{2}{3}}\bar{T}_1 = \frac{T}{T_\infty} - 1 < \frac{s_{v\infty} - s_g(T_\infty)}{T_\infty(ds_g/dT)_\infty\{1 - [s_g(T_\infty) - s_{v\infty}]/s_{fg}(T_\infty)\}}$$

Of specific interest is the case where the relative humidity of the freestream flow is $\Phi_\infty = 100\%$ [the thermodynamic condition where the pressure of water vapor p_v in the freestream equals the saturation pressure $p_g(T_\infty)$]. Then, $s_{v\infty} = s_g(T_\infty)$,

$$\bar{g}_1 = \epsilon^{\frac{2}{3}}\frac{\bar{T}_1 T_\infty}{s_{fg}(T_\infty)}\left(\frac{ds_g}{dT}\right)_\infty \tag{25}$$

when $\bar{T}_1 < 0$, and $\bar{g}_1 = 0$ when $\bar{T}_1 \ge 0$. In this case, $\bar{g}_1$ is generated only when the temperature decreases below T_∞. Also note that when $M_\infty \sim 1$ and $\Phi_\infty \sim 100\%$ the condensation region is close to the supersonic region in the floor and can be used to identify it as a floor visualization technique (see the pictures in Refs. 2 and 3).

Using Eqs. (21) and (24), we find that Eq. (22) may be given in the following form:

$$\left[K - (\gamma_a + 1)M_\infty^2\phi_{1\bar{x}}\right]\phi_{1\bar{x}\bar{x}} + \left\{\epsilon^{\frac{2}{3}}K_\omega M_\infty^2\left[\frac{h_{fg}(T_\infty)}{C_{pa}T_\infty} - \frac{\mu_a}{\mu_v}\right]\frac{(\gamma_a - 1)T_\infty}{s_{fg}(T_\infty)}\left(\frac{ds_g}{dT}\right)_\infty \times\left[1 - \frac{s_g(T_\infty) - s_{v\infty}}{s_{fg}(T_\infty)}\right]H(\phi_{1\bar{x}})\right\}\phi_{1\bar{x}\bar{x}} + \phi_{1\bar{y}\bar{y}} = 0 \tag{26}$$

where, $H(z)$ is the Heaviside function, that is, $H(z) = 1$ when $z > 0$ and $H(z) = 0$ when $z \le 0$. The term in Eq. (26) with the condensation effect (with the Heaviside function) is active only when $\phi_{1\bar{x}} > 0$, that is, when the axial speed exceeds the freestream uniform speed. The solution of Eq. (26) must satisfy the boundary and far-field conditions described by Eq. (23).

Equation (26) shows that the flow of moist air with freestream frozen Mach number M_∞ and temperature T_∞ around an airfoil with thickness ratio ϵ is close in its behavior to the flow of dry air around the same airfoil with an effective freestream Mach number $\bar{M}_\infty$, which can approximately be computed from the requirement

$$\bar{M}_\infty^2 = 1 - \bar{K}\epsilon^{\frac{2}{3}} \tag{27}$$

where

$$\bar{K} = K + \epsilon^{\frac{2}{3}}K_\omega M_\infty^2\left[\frac{h_{fg}(T_\infty)}{C_{pa}T_\infty} - \frac{\mu_a}{\mu_v}\right]\frac{(\gamma_a - 1)T_\infty}{s_{fg}(T_\infty)} \times\left(\frac{ds_g}{dT}\right)_\infty\left[1 - \frac{s_g(T_\infty) - s_{v\infty}}{s_{fg}(T_\infty)}\right]$$

Note that because $(ds_g/dT)_\infty < 0$ for every T_∞, the effective freestream Mach number $\bar{M}_\infty > M_\infty$. This means that the humidity effects may act similarly to the increase of the freestream Mach number in a dry airflow case.

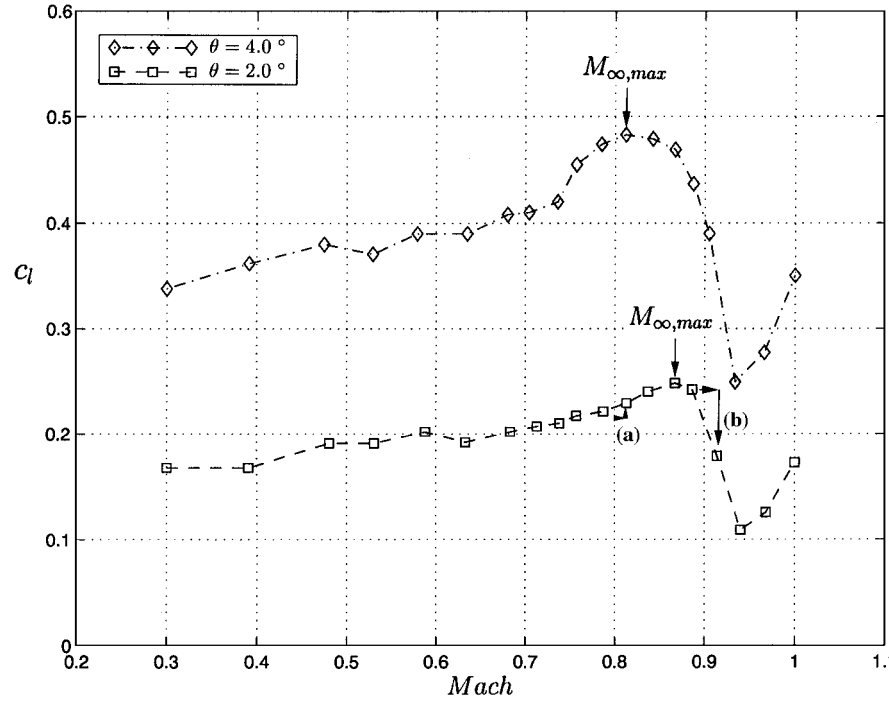

Fig. 2 Change of lift coefficient with Mach number along a NACA 64A009 airfoil at various angles of attack.

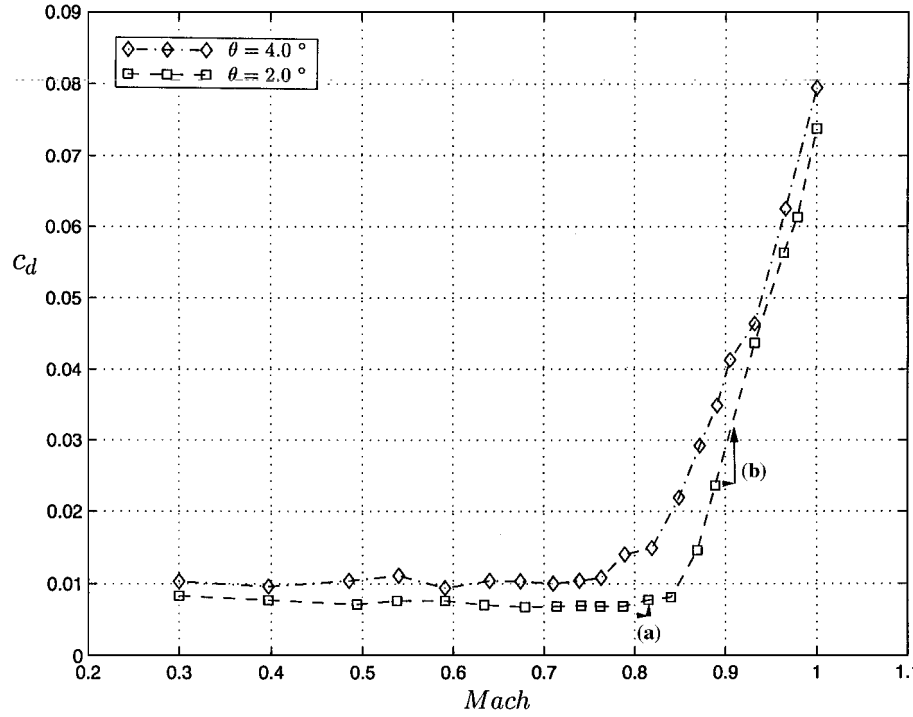

Fig. 3 Change of drag coefficient with Mach number along a NACA 64A009 airfoil at various angles of attack.

To better understand the effect of the humidity in atmospheric moist air as it is represented by the effective freestream Mach number, we refer to the representative experimental data for the flow of dry air shown in Figs. 2–4. Figures 2–4 describe the change of the lift, drag, and pitching moment coefficients of a NACA 64A009 airfoil with freestream Mach number for various fixed angles of attack (the data are taken from McCormick,[23] page 215). It can be seen that for each angle of attack there exists a Mach number $M_{\infty,\max}$ for which the lift coefficient reaches a maximum value. For a NACA 64A009, $M_{\infty,\max} \sim 0.87$ when $\theta = 2$ deg and $M_{\infty,\max} \sim 0.82$ when $\theta = 4$ deg. Typically, when $M_\infty < M_{\infty,\max}$ and $\bar{M}_\infty < M_{\infty,\max}$, the effect of humidity in moist air may be to increase the lift coefficient together with drag increase and with nose-down change in pitching moment (Case (a) in Figs. 2–4). On the other hand, when $M_\infty > M_{\infty,\max}$, the effect of humidity in moist air may be to significantly decrease the lift coefficient together with a large increase of drag and with nose-up change in pitching moment (Case (b) in Figs. 2–4). For example, according to the present theory, the flow of moist air with $\Phi_\infty = 100\%$ and $T_\infty = 293.15$ K [at these conditions, from Eq. (2), $\omega_\infty = 0.0145$] at $M_\infty = 0.8$, which is below $M_{\infty,\max} = 0.87$, around a NACA 64A009 airfoil at $\theta = 2$ deg is similar to the flow of dry air at an effective Mach number $\bar{M}_\infty = 0.812$ around the same airfoil at

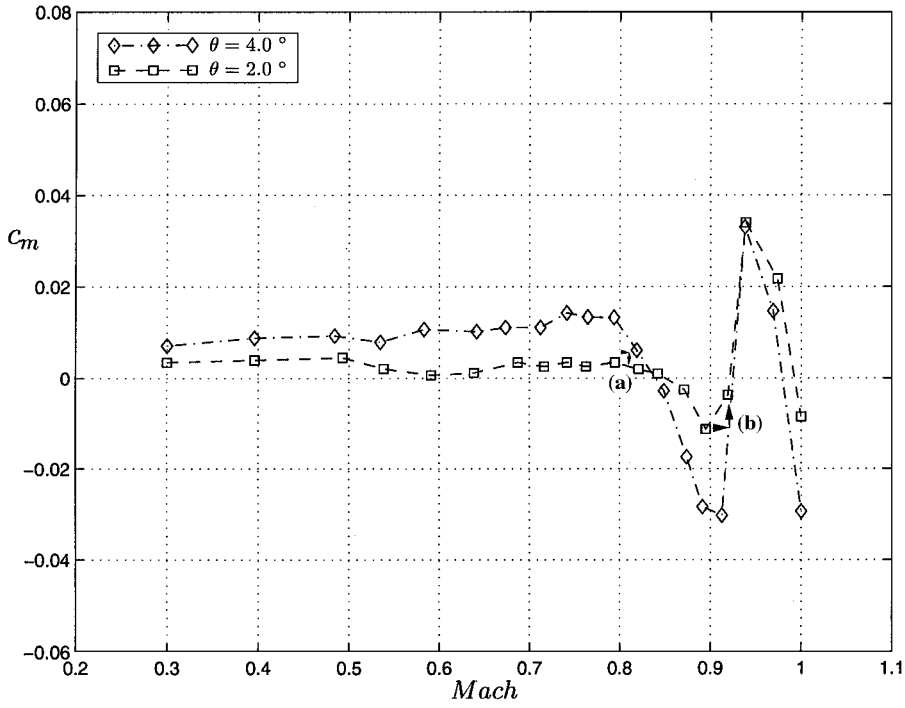

Fig. 4 Change of pitching moment coefficient with Mach number along a NACA 64A009 airfoil at various angles of attack.

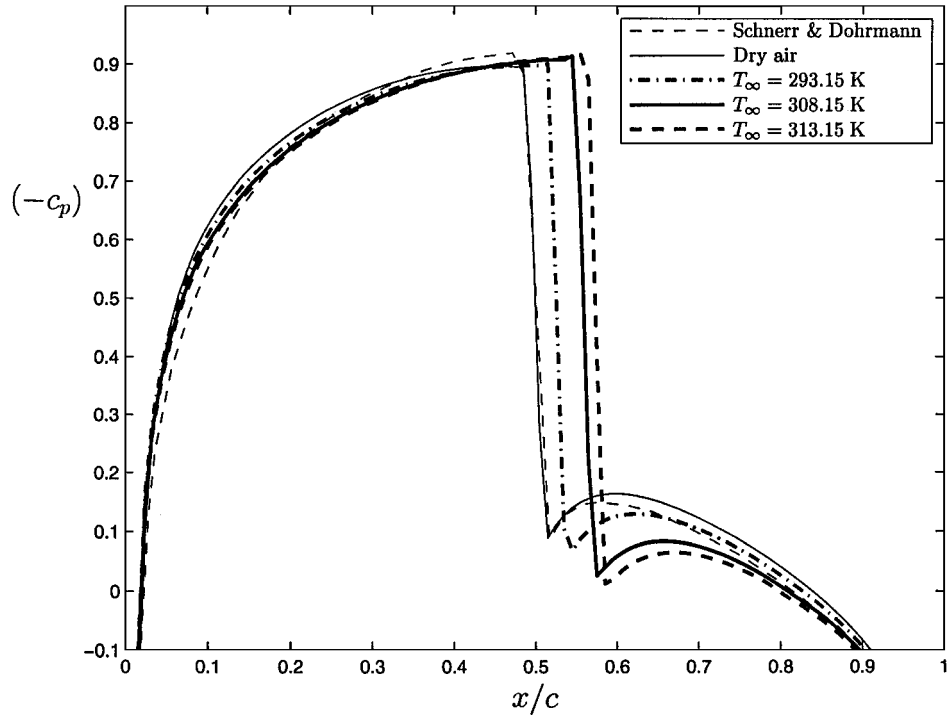

Fig. 5 Distribution of pressure coefficient along a NACA 0012 airfoil at zero angle of attack with $M_\infty = 0.8$ and $\Phi_\infty = 100\%$ for various freestream temperatures.

same $\theta = 2$ deg. This may result for the moist airflow in the increase of lift with about 2% and of drag with about 6% against the dry air case. On the other hand, according to the present theory, the flow of moist air with a relative humidity of $\Phi_\infty = 100\%$ and $T_\infty = 293.15$ K [at these conditions, from Eq. (2), $\omega_\infty = 0.0145$] at $M_\infty = 0.89$ around a NACA 64A009 at $\theta = 2$ deg is similar to the flow of dry air at an effective Mach number $\bar{M}_\infty = 0.905$ around the same airfoil at same $\theta = 2$ deg. This may result for the moist airflow in the decrease of lift with about 18% and increase of drag with about 32% against the dry air case. These examples also demonstrate the use of the present theory together with wind-tunnel data for dry air to predict aerodynamic performance of airfoils in moist air. In a similar way, the theory can be used with numerical results of flows of dry air to estimate the humidity effects.

IV. Numerical Studies

The problem of Eq. (26) with conditions of Eq. (23) can be solved numerically using Murman and Cole's[21] method. According to this technique, a test is developed to identify the type of every computational grid point. At each step of the iterations, the computations use the suitable difference scheme at that point. A central-differencescheme is used for the $\bar{x}$ derivativesof ϕ_1 when the

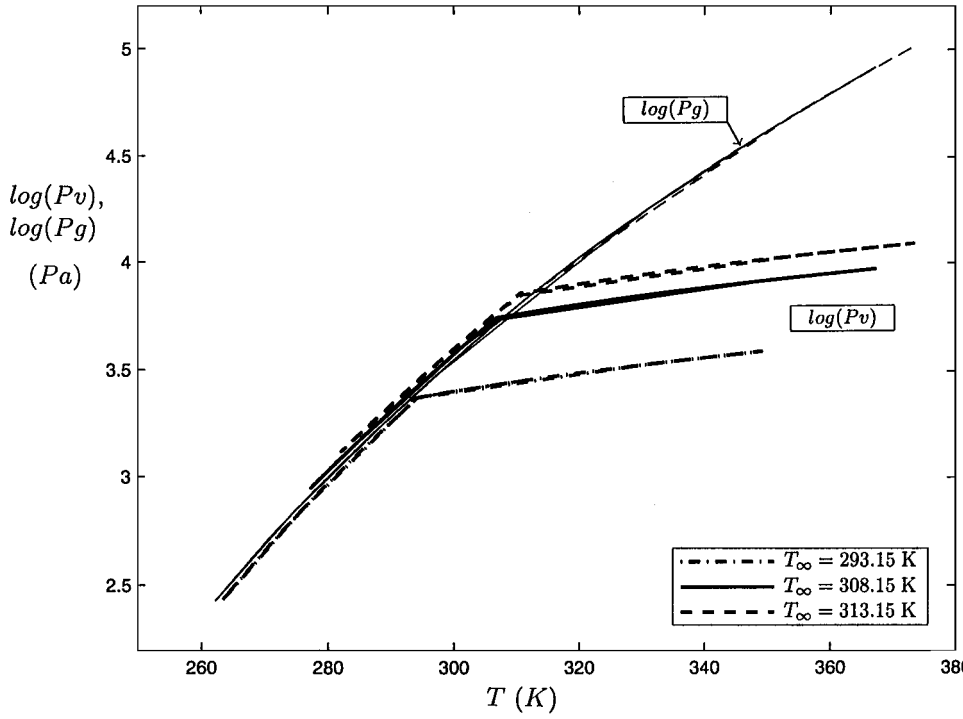

Fig. 6 Change of vapor pressure along a stream line that runs close to the airfoil in a p–T phase diagram at zero angle of attack with $M_\infty = 0.8$ and $\Phi_\infty = 100\%$ for various freestream temperatures.

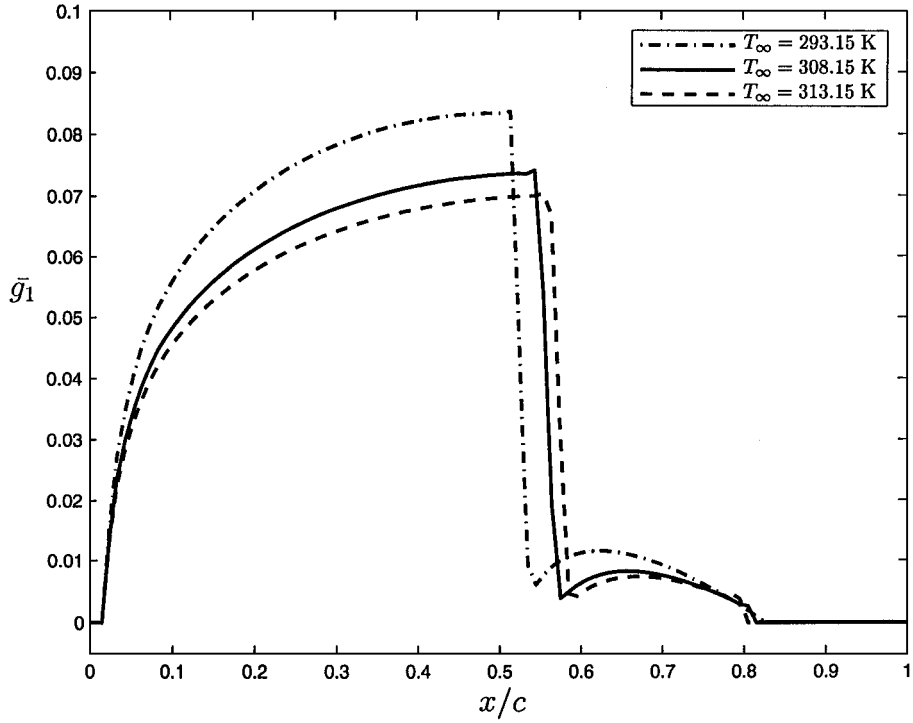

Fig. 7 Distribution of condensate mass fraction along a NACA 0012 airfoil at zero angle of attack with $M_\infty = 0.8$ and $\Phi_\infty = 100\%$ for various freestream temperatures.

equation at a grid point is elliptic (subsonic), a backward-difference scheme is used when the equation at a grid point is hyperbolic (supersonic), and a mixed-type-differencescheme is used when a shock wave appears at a grid point. Also, a central-difference scheme is always used for the $\tilde{y}$ derivatives. The flow tangency condition along the airfoil chord is applied at grid points near the airfoil segment. Nonreflective conditions are applied along the boundaries of the computational domain. The computations are repeated until the solution of Eq. (26) with Eq. (23) converges to a steady-state solution. Then, the pressure coefficient along the airfoil's surfaces, $c_p = -2\epsilon^{2/3}\phi_{1\tilde{x}}$, and the field of the condensate mass fraction, $\bar{g}_1$, are computed.

Figures 5–7 describe the numerical solution of a transonic flow of moist air with a freestream frozen Mach number $M_\infty = 0.8$ and relative humidity $\Phi_\infty = 100\%$ (saturated air). Three cases of temperatures $T_\infty = 293.15$ (sea-level standard temperature), 308.15, and 313.15 K were studied. In all of these cases, the flow around a NACA 0012 airfoil at zero angle of attack is considered. It can be seen from Fig. 5 that the dry air solution agrees with solutions of the Euler equations.[4] Figure 5 also shows that the pressure coefficient

along the airfoil changes due to the change of the temperature T_∞. Specifically, the shock wave position moves downstream as the freestream temperature increases. These changes result in the increase of the pressure drag. Figure 6 describes in the p–T phase diagram the change of the water vapor pressure along a streamline that runs from upstream infinity and near the airfoil surface. It can be seen that the water vapor pressure follows same line and also matches with the saturation pressure when saturation conditions occur. This indicates that the process of condensation in the computations is indeed isentropic. Figure 7 shows the distribution of the condensate mass fraction along the airfoil surface for the various cases. It can be seen that the distribution of $\bar{g}_1$ along the airfoil is similar to that of the negative of the pressure coefficient, $-c_p$, along the airfoil (comparing Fig. 5 with Fig. 7). This is consistent with Eqs. (21) and (25), which show that when the relative humidity is 100% the condensate mass fraction is related to the pressure perturbation,

$$\bar{g}_1 = \frac{(\gamma_a - 1)T_\infty}{2s_{fg}(T_\infty)}\left(\frac{\mathrm{d}s_g}{\mathrm{d}T}\right)_\infty M_\infty^2 c_p$$

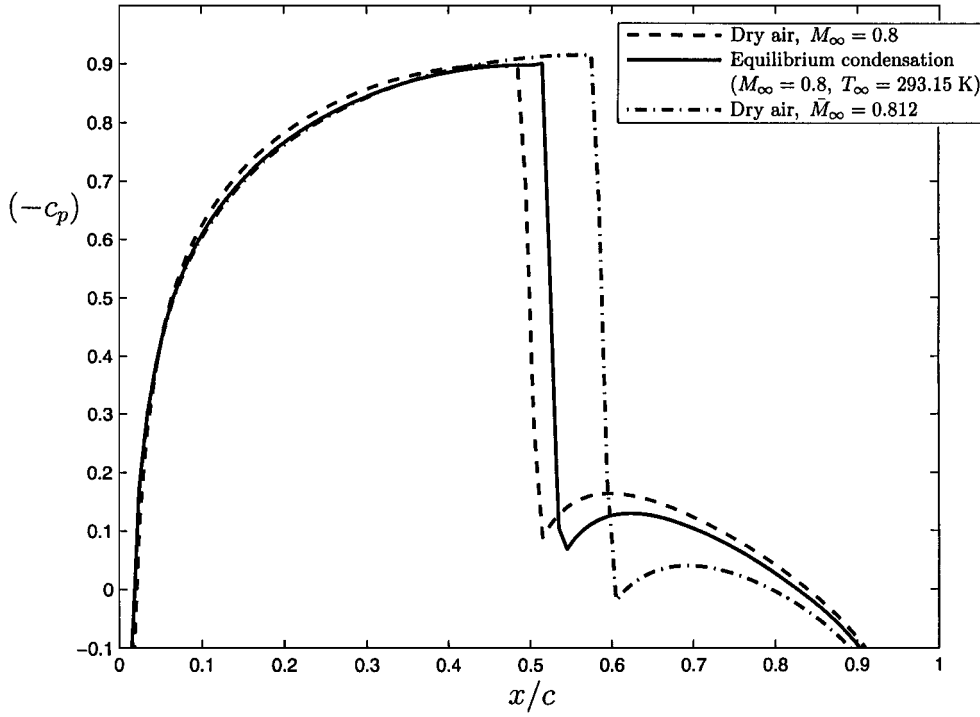

Fig. 8 Distribution of pressure coefficient along a NACA 0012 airfoil for two self-similar cases.

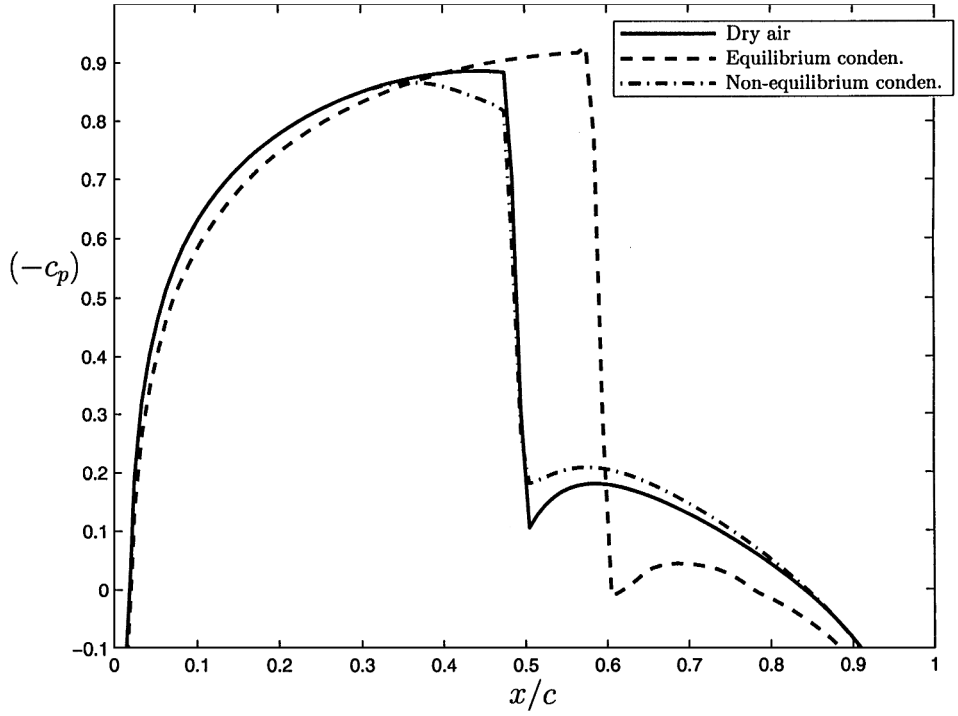

Fig. 9 Distributions of pressure coefficient along a NACA 0012 at zero angle of attack and $M_\infty = 0.8$ for equilibrium and nonequilibrium condensation.

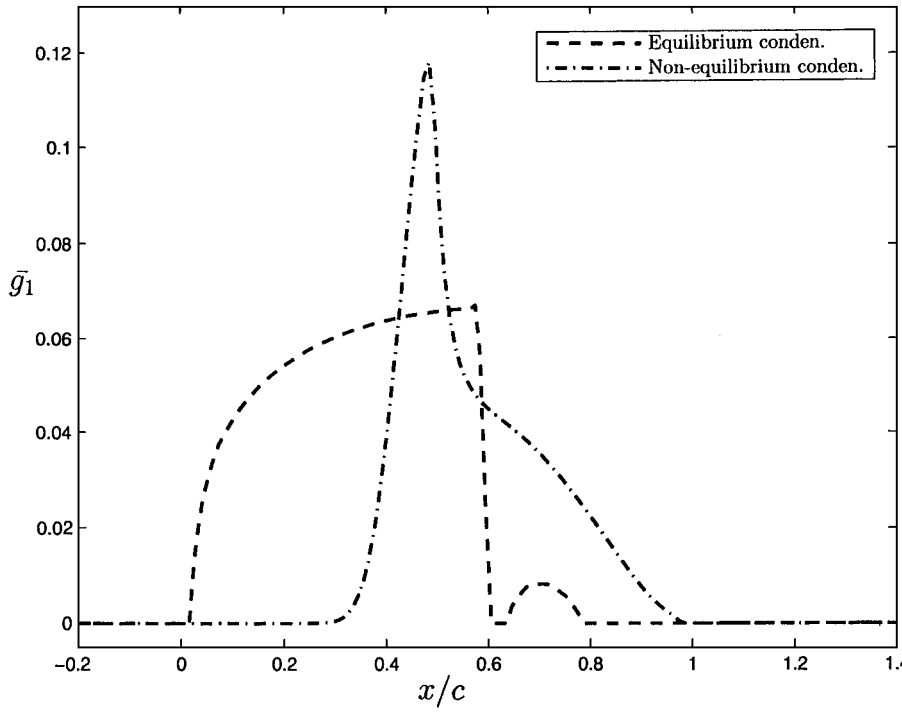

Fig. 10 Distributions of condensate mass fraction along a NACA 0012 at zero angle of attack and $M_\infty = 0.8$ for equilibrium and nonequilibrium condensation.

The values of $\bar{g}_1$ decrease with the increase of T_∞ because $T_\infty / s_{fg}(T_\infty)(\mathrm{d}s_g/\mathrm{d}T)_\infty$ decreases in its absolute value with the increase of T_∞ (see Ref. 22).

Figure 8 shows the distribution of the pressure coefficient along a NACA 0012 airfoil for three cases. The first case is of a flow of dry air with $M_\infty = 0.8$ around a NACA 0012 at zero angle of attack. The second case is of a flow of moist air with $T_\infty = 293.15$ K and $\Phi_\infty = 100\%$, and the third case is of a flow of dry air with an effective freestream Mach number $\bar{M}_\infty = 0.812$, which corresponds to the second case according to Eq. (27). The results show that the flow of moist air is close to the flow of dry air with the increased freestream Mach number. However, the similarity between the two cases is incomplete because the humidity effects included in Eq. (26) are limited to the regions in the flowfield where $\phi_{1\bar{x}} > 0$.

Figures 9 and 10 show a comparison of computed results for two flows of moist air; one is with equilibrium condensation and the other is with nonequilibrium and homogeneous condensation. The present theory is used to predict the moist air behavior with equilibrium condensation. The theory of Rusak and Lee[17] is used to predict the moist air behavior with nonequilibrium and homogeneous condensation. In both cases, we study a uniform flow of saturated air with $\Phi_\infty = 100\%$, $T_\infty = 318.15$ K, and $M_\infty = 0.8$ around a NACA 0012 airfoil with chord of $c = 4$ m at zero angle of attack. The results of the distribution of the pressure coefficient (Fig. 9) and the condensate mass fraction (Fig. 10) along the airfoil surface demonstrate that the two processes of condensation that occur around the airfoil are very different in their mechanism and effect on the aerodynamic performance of the airfoil. In the equilibrium condensation, the process starts immediately as the saturation conditions are achieved, whereas in the nonequilibrium and homogeneous condensation, the process starts only after a supersaturation state at a critical low temperature is achieved. In the equilibrium condensation, the condensate mass fraction is similar to the negative of the pressure coefficient and has a moderate buildup, whereas in the nonequilibrium condensation, there is no such an explicit relation and the condensate suddenly appears at the critical condition. In the examples studied here, the effect of the equilibrium condensation causes the shock wave to shift downstream and increase the pressure drag against the dry air case, whereas the effect of nonequilibrium condensation is local, occurs ahead of the shock wave, and results in a relatively small compression wave with only a slight change of shock wave position and of the airfoil's pressure drag. Also, a comparison of the theory developed in this paper with that by Rusak and Lee[17] shows that the flow of moist air with equilibrium condensation is independent of the airfoil's chord in contrast to the flow of moist air with nonequilibrium condensation, which is strongly dependent on the airfoil's chord.

V. Conclusions

The two-dimensional and steady transonic flow of atmospheric moist air with equilibrium (isentropic) condensation around a thin airfoil can be studied by an asymptotic analysis. A small-disturbance model can be formulated to represent the nonlinear interactions between the near-sonic speed of the flow, the small thickness ratio and angle of attack of the airfoil, and the small amount of mass of water vapor in the air. The condensate mass fraction can be expressed in terms of the velocity potential. The problem is governed by two similarity parameters. One is the classical transonic parameter K, which defines the deviation of the freestream speed from the sonic speed in terms of the thickness ratio of the airfoil. The other is the humidity parameter K_ω, which defines the amount of mass of water vapor in the air in terms of the thickness ratio of the airfoil. The flowfield may be described by an extended TSD equation that includes parameters that are related to the condensation process. The extended TSD equation can be solved numerically by Murman and Cole's[21] method. The results show that the flow of moist air is similar to the flow of dry air with an effective freestream Mach number. It is found that for all temperatures $\bar{M}_\infty > M_\infty$. The present approach demonstrates the change of the aerodynamic performance of airfoils in atmospheric transonic flight due to the humidity effects. The theoretical approach can be used together with experimental data or results of simulations for flows of dry air to predict the lift, drag, and pitching moment coefficients of airfoils operating in atmospheric moist air. The condensation regions may also be used to identify the supersonic speed regions in the flow.

References

[1] Wegener, P. P., and Pouring, A. A., "Experiments on Condensation of Water Vapor by Homogeneous Nucleation in Nozzles," *Physics of Fluids,* Vol. 7, No. 3, 1964, pp. 352–361.

[2]Campbell, J. F., Chambers, J. R., and Rumsey, C. L., "Observation of Airplane Flowfields by Natural Condensation," *Journal of Aircraft*, Vol. 26, No. 7, 1989, pp. 593–604.

[3]Gay, J., "Going Supersonic," *Life*, Jan. 2000, pp. 70, 71.

[4]Schnerr, G. H., and Dohrmann, U., "Transonic Flow Around Airfoils with Relaxation and Energy Supply by Homogeneous Condensation," *AIAA Journal*, Vol. 28, No. 7, 1990, pp. 1187–1193.

[5]Schnerr, G. H., and Dohrmann, U., "Drag and Lift in Nonadiabatic Transonic Flow," *AIAA Journal,* Vol. 32, No. 1, 1994, pp. 101–107.

[6]Head, R., "Investigation in Spontaneous Condensation Phenomena," Ph.D. Dissertation, Dept. of Aeronautical Engineering, California Inst. of Technology, Pasadena, CA, 1949.

[7]Wegener, P. P., and Mack, L. M., "Condensation in Supersonic and Hypersonic Wind Tunnels," *Advances in Applied Mechanics,* edited by H. L. Dryden and T. von Kármán, Academic, New York, Vol. 5, 1958, pp. 307–447.

[8]Schmidt, B., "Schallnahe profilumströmungen mit kondensation," *Acta Mechanica,* Vol. 2, No. 2, 1966, pp. 194–208.

[9]Zierep, J., "Schallnahe strömungen mit wärmezufuhr," *Acta Mechanica*, Vol. 8, No. 1–2, 1969, pp. 126–132.

[10]Zierep, J., *Similarity Laws and Modeling, Gasdynamics Series of Monographs,* edited by P. P. Wegener, Marcel Dekker, New York, 1971.

[11]Jordan, F. L., "Investigation at Near-Sonic Speed of Some Effects of Humidity on the Longitudinal Aerodynamic Characteristics of a NASA Supercritical Wing Research Airplane Model," NASA TM X-2618, 1972.

[12]Hall, R. M., "Onset of Condensation Effects with an NACA 0012-64 Airfoil Tested in the Langley 0.3-Meter Transonic Cryogenic Wind Tunnel Technology," NASA TP 1385, 1979.

[13]Schnerr, G. H., and Mundinger, G., "Similarity, Drag and Lift in Transonic Flow with Given Internal Heat Addition," *European Journal of Mechanics, B/Fluids,* Vol. 12, No. 5, 1993, pp. 597–612.

[14]Wegener, P. P., "Nonequilibrium Flow with Condensation," *Acta Mechanica,* Vol. 21, No. 1–2, 1975, pp. 65–91.

[15]Zettlemoyer, A. C., *Nucleation,* Marcel Dekker, New York, 1969.

[16]Abraham, F. F., *Homogeneous Nucleation Theory,* Academic, New York, 1974.

[17]Rusak, Z., and Lee, J. C., "Transonic Flow of Moist Air Around a Thin Airfoil with Nonequilibrium and Homogeneous Condensation," *Journal of Fluid Mechanics,* Vol. 403, 2000, pp. 173–199.

[18]Lee, J. C., and Rusak, Z., "Nonadiabatic Compressible Flow of Humid Air Around Airfoil," *Advances in Fluid Mechanics*, edited by M. Rahman and C. A. Brebbia, Vol. 3, 2000, pp. 323–333.

[19]Lee, J. C., "Transonic Flow of Moist Air Around Thin Airfoils," Ph.D. Dissertation, Dept. of Mechanical Engineering, Astronautical Engineering and Mechanics, Rensselaer Polytechnic Inst., Troy, NY, April 2000.

[20]Cole, J. D., and Cook, L. P., *Transonic Aerodynamics,* North-Holland, Amsterdam, 1986, Chap. 3.

[21]Murman, E. M., and Cole, J. D., "Calculation of Plane Study Transonic Flows," *AIAA Journal*, Vol. 9, No. 1, 1971, pp. 114–121.

[22]Moran, M. J., and Shapiro, H. N., *Fundamentals of Engineering Thermodynamics*, 3rd ed., Wiley, New York, 1992, Chap. 12.

[23]McCormick, B. W., *Aerodynamics, Aeronautics, and Flight Mechanics*, 2nd ed., Wiley, New York, 1995, pp. 214, 215.